

# Cross-orientation masking in human color vision: Application of a two-stage model to assess dichoptic and monocular sources of suppression

Yeon Jin Kim

McGill Vision Research, Department of Ophthalmology,  
McGill University, Montreal, Quebec, Canada



Mina Gheiratmand

McGill Vision Research, Department of Ophthalmology,  
McGill University, Montreal, Quebec, Canada



Kathy T. Mullen

McGill Vision Research, Department of Ophthalmology,  
McGill University, Montreal, Quebec, Canada



**Cross-orientation masking (XOM) occurs when the detection of a test grating is masked by a superimposed grating at an orthogonal orientation, and is thought to reveal the suppressive effects mediating contrast normalization. Medina and Mullen (2009) reported that XOM was greater for chromatic than achromatic stimuli at equivalent spatial and temporal frequencies. Here we address whether the greater suppression found in binocular color vision originates from a monocular or interocular site, or both. We measure monocular and dichoptic masking functions for red-green color contrast and achromatic contrast at three different spatial frequencies (0.375, 0.75, and 1.5 cpd, 2 Hz). We fit these functions with a modified two-stage masking model (Meese & Baker, 2009) to extract the monocular and interocular weights of suppression. We find that the weight of monocular suppression is significantly higher for color than achromatic contrast, whereas dichoptic suppression is similar for both. These effects are invariant across spatial frequency. We then apply the model to the binocular masking data using the measured values of the monocular and interocular sources of suppression and show that these are sufficient to account for color binocular masking. We conclude that the greater strength of chromatic XOM has a monocular origin that transfers through to the binocular site.**

## Introduction

Contrast gain control has been widely studied psychophysically using measurements of cross-orienta-

tion masking (XOM), in which the detection of a test stimulus, such as a grating, is masked by a superimposed stimulus at an orthogonal orientation (Ross & Speed, 1991; Foley, 1994; Chen & Foley, 2004; Holmes & Meese, 2004; Petrov, Carandini, & McKee, 2005; Baker, Meese, & Summers, 2007; Meese, Summers, Holmes, & Wallis, 2007; Cass, Stuit, Bex, & Alais, 2009). XOM is usually attributed to inhibitory interactions between separate neural detectors each tuned to a different orientation, sometimes called a “cross-channel” effect. This inhibitory interaction is considered to be a contrast gain control, and has been described by a number of contrast normalization models in which there is divisive inhibition from a broad pool of detectors operating on the response to the test stimulus (Geisler & Albrecht, 1992; Heeger, 1992; Foley, 1994; Brouwer & Heeger, 2011). Through this process, cortical neurons can effectively respond to a wide range of contrasts and maintain stimulus selectivity. Cross-orientation suppression (XOS) is observed in most neurons in mammalian cortex (Morrone, Burr, & Maffei, 1982; Bonds, 1989; DeAngelis, Robson, Ohzawa, & Freeman, 1992; Heeger, 1992; Carandini, Heeger, & Movshon, 1997; Walker, Ohzawa, & Freeman, 1998; Li, Peterson, Thompson, Duong, & Freeman, 2005; Sengpiel & Vorobyov, 2005). While the origin of XOS is thought to be primarily cortical, there is also evidence in the cat indicating the involvement of subcortical, monocular sites (Walker et al., 1998; Truchard, Ohzawa, & Freeman, 2000; Carandini, Heeger, & Senn, 2002; Freeman, Durand, Kiper, & Carandini, 2002; Li et al., 2005; Sengpiel & Vorobyov, 2005; Priebe &

Citation: Kim, Y. J., Gheiratmand, M., & Mullen, K. T. (2013). Cross-orientation masking in human color vision: Application of a two-stage model to assess dichoptic and monocular sources of suppression. *Journal of Vision*, 13(6):15, 1–14, <http://www.journalofvision.org/content/13/6/15>, doi:10.1167/13.6.15.

Ferster, 2006), and overall, it is likely that multiple sites contribute to the psychophysical effect.

Psychophysically, XOM for achromatic stimuli has been shown to have a characteristic spatiotemporal selectivity, with the highest masking found for low spatial frequency stimuli presented at high temporal frequencies, and least masking for high spatial frequencies at low temporal frequencies (Meese & Holmes, 2007). This suggested that XOM may be associated with the subcortical, magnocellular pathway or its cortical projections. To test this hypothesis, Medina and Mullen (2009) compared XOM for binocularly presented achromatic and isoluminant red-green stimuli at equivalent spatial and temporal frequencies (0.375–1.5 cpd, 2–8 Hz) and found suppression was significantly greater for the chromatic stimuli. Since red-green stimuli are detected exclusively by the parvocellular pathway of the lateral geniculate nucleus (LGN), this indicates that XOS is as strong in the chromatic parvocellular pathway and its projections as in the magnocellular pathway, and suggests that XOS is not confined to one specific subcortical pathway.

In this paper, we return to the issue of XOM in color vision. Psychophysical models developed previously for luminance contrast have proposed that two sources of XOS occur before binocular summation: a site of suppression acting on signals originating monocularly within each eye, and a dichoptic, interocular route, in which signals from the two eyes mutually suppress each other (Meese & Hess, 2004; Baker et al., 2007; Meese & Baker, 2009). Marked differences between these two types of suppression in terms of their spatiotemporal tuning, the effect of stimulus duration, and response to adaptation suggests that they reflect different mechanisms of suppression operating at different sites (Baker et al., 2007). Here we address whether the greater XOM found in binocular color vision compared to luminance vision originates from a monocular site, an interocular site, or is found equally in both of these. We measure monocular, dichoptic, and binocular masking functions for color and achromatic contrast across a range of spatial frequencies. We fit the monocular and dichoptic functions with a modified two-stage masking model (Foley, 1994; Meese & Holmes, 2007; Meese & Baker, 2009), and extract the dichoptic and monocular weights of suppression. We compare the relative strengths of these two sources of suppression in color vision and in luminance vision under equivalent conditions. We then apply the model to our binocular masking data. We demonstrate that the two measured sources of suppression prior to binocular summation, one interocular and one monocular, are sufficient to predict the color binocular masking functions.

## Methods

### Apparatus

Stimuli were generated by a ViSaGe video-graphics card (Cambridge Research Systems, Kent, UK) with 14-bit contrast resolution and presented on a Sony Trinitron (GDM 500DIS) monitor (Sony Corporation, Tokyo, Japan) at 120 Hz frame rate and  $1024 \times 768$  spatial resolution. The gamma correction was performed using the VSG calibration routine with the OptiCal photometer (Cambridge Research Systems). The spectral emission functions of the red, green, and blue phosphors of the monitor were measured using a Spectra Scan PR-645 spectrophotometer (Photo Research Inc., Chatsworth, CA). The CIE-1931 chromaticity coordinates of the red, green, and blue phosphors were ( $x = 0.610, y = 0.333$ ), ( $x = 0.302, y = 0.591$ ), and ( $x = 0.153, y = 0.084$ ), respectively. The background was achromatic with a mean luminance of  $51 \text{ cd/m}^2$  at the screen center. All stimuli were viewed through a mirror stereoscope in a dimly lit room with a viewing distance of 58 cm.

### Observers

Four subjects participated in this study: three authors (YJK, MG, and KTM) and one naive subject (JWZ). All subjects had normal or corrected-to-normal visual acuity and normal color vision. The experiments were performed in accordance with the Declaration of Helsinki.

### Color space

Stimuli were represented in a three-dimensional cone-contrast space (Cole, Hine, & McIlhagga, 1993; Sankeralli & Mullen, 1996) in which each axis is defined by the incremental stimulus intensity for each cone type to a given stimulus normalized by the respective intensity of the fixed adapting white background. Cone excitations for the L-, M-, and S-cones were calculated using the cone fundamentals of Smith and Pokorny (1975). A linear transform was calculated to specify the required phosphor contrasts of the monitor for given cone contrasts. Postreceptoral luminance and red-green cone-opponent mechanisms were modeled as linear combinations of cone contrast responses and were isolated by using achromatic ( $L + M + S$ ) and isoluminant red-green ( $L - aM$ ) cardinal stimuli, where  $a$  is a numerical constant obtained at isoluminance. Stimulus contrast is defined as the vector length in cone contrast units ( $C_C$ ):

$$C_C = \sqrt{(L_C)^2 + (M_C)^2 + (S_C)^2} \quad (1)$$

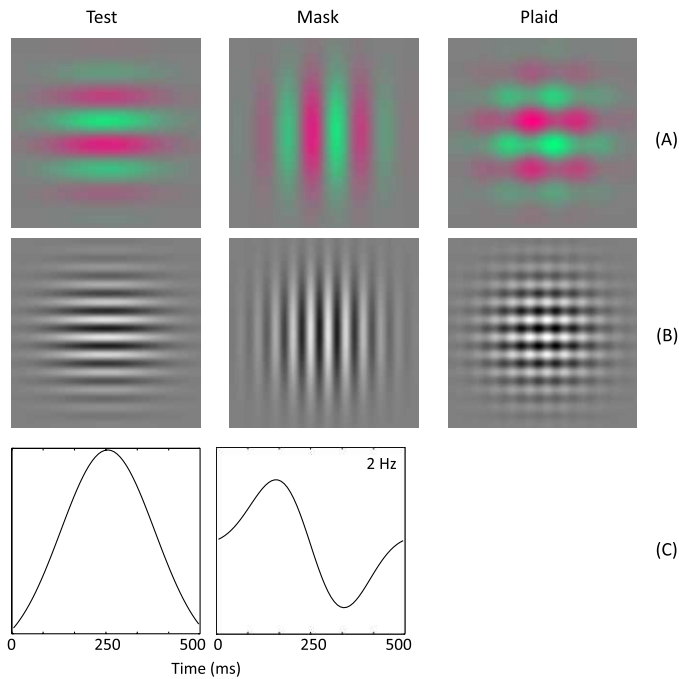


Figure 1. All stimuli were Gabors with a fixed space constant of  $\sigma = 2^\circ$ . (A) An example of the red-green isoluminant Gabors (0.375 cpd) used for the horizontal test stimulus and the vertical mask stimulus, with their superimposition at high contrasts (plaid). (B) shows the same as (A) but for an achromatic Gabor (1.5 cpd). (C) Left, the Gaussian temporal envelope used to modulate the contrast of the test and mask stimuli ( $\sigma = 125$  ms, in a window of 500 ms duration). Right, the temporal envelope multiplied by the sinusoidal temporal waveform (2 Hz).

where  $L_c$ ,  $M_c$ , and  $S_c$  represent the L, M, and S Weber cone-contrast fractions in relation to the L-, M-, and S-cone values of the achromatic background. This metric differs by a factor of  $\sqrt{3}$  from the conventional luminance contrast. For each observer and for each spatial and temporal frequency, the isolation of the red-green mechanism at isoluminance (value of  $a$  above) was estimated by a minimum motion task (Cavanagh, Tyler, & Favreau, 1984), in which the perceived minimum motion of the Gabor was measured using a method of adjustment and was based on the average of at least 10 settings.

## Stimuli

Both chromatic and achromatic test stimuli were horizontally oriented Gabor patterns. The mask stimuli were overlaid and spatially orthogonal to the test (vertical), with the same spatiotemporal frequency, phase, and color properties as the test stimulus. Three different spatial frequencies were used (phase = 0):

0.375, 0.75, and 1.5 cpd (see Figure 1A and B). The Gaussian envelopes of the Gabor stimuli were scaled to a fixed space constant ( $\sigma = 2^\circ$ ). Gabors were sinusoidally phase reversed in time at 2 Hz. All Gabors were presented in a contrast modulated temporal Gaussian envelope ( $\sigma = 125$  ms, see Figure 1C). Both test and mask stimuli were controlled independently by lookup tables and were interlaced with frame-by-frame cycling. The maximum mask contrast was limited by the color gamut of the monitor and the frame interleaving. Test and mask were presented under monocular, dichoptic, and binocular viewing conditions using the stereoscope. In the monocular condition, the test and mask gratings were both presented to the right eye. In the binocular condition, the test and mask gratings were presented to both eyes. In the dichoptic condition, the test was presented to the right eye and the mask to the left eye.

## Procedure

We first measured contrast detection thresholds for both the horizontal and vertical orientations in the absence of a mask. We then measured contrast detection thresholds for the horizontal test stimuli in the presence of the overlaid vertical mask stimulus at a fixed cone contrast. Thresholds were measured using a two-interval forced-choice (2IFC) staircase procedure, a “2-down, 1-up” weighted staircase with audio feedback. Presentation intervals were 500 ms each, separated by 500 ms. Subjects indicated with a button-press in which interval the test stimulus appeared. A reversal was defined when the subject responded incorrectly after a minimum of two consecutive correct responses. Each staircase terminated after six reversals. After the first reversal, stimulus contrast was raised by 25% following one incorrect response and lowered by 12.5% following two consecutive correct responses. For any given staircase session, the number of total trials fluctuated between approximately 35 and 65. The threshold value was calculated as the arithmetic mean of the last five reversals of the staircase (81.6% correct detection level). Thresholds were measured in a block design. In one block, thresholds at all mask contrasts (low to high) in one viewing condition (monocular, dichoptic, or binocular) were measured. The order of the blocks was pseudorandom. Each block was repeated at least four times over the course of the experiment; hence each plotted threshold is based on the arithmetic mean of a minimum of four staircase measurements. Data for different spatial frequencies were collected in different experiments, each using the same block design.

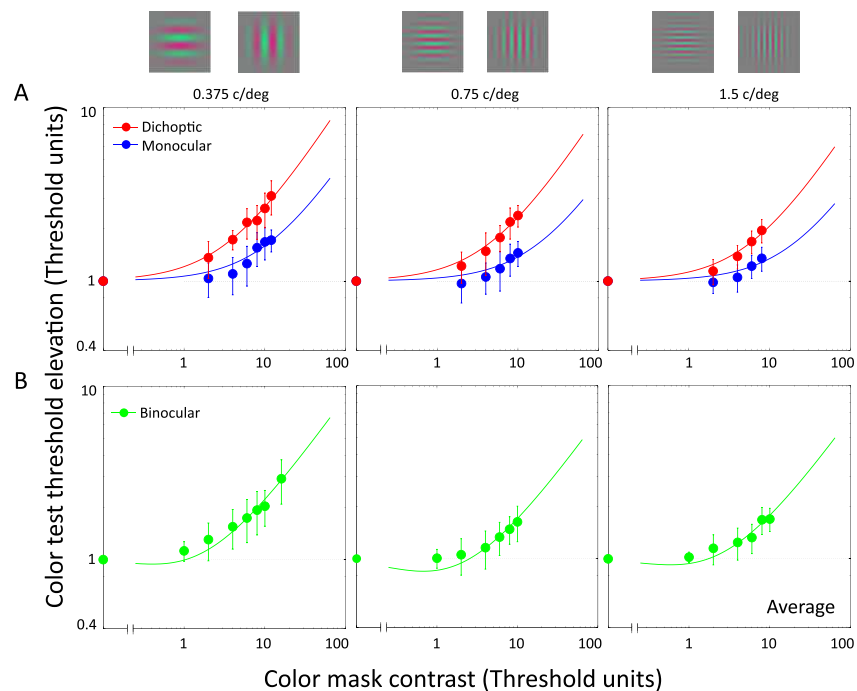


Figure 2. Threshold elevation of the test stimulus plotted as a function of the orthogonal mask contrast (TvC functions) for chromatic stimuli for three viewing conditions: (A) monocular (blue symbols) and dichoptic (red symbols) and (B) binocular (green symbols). Results are the average across four subjects (KTM, JWZ, MG, and YJK). Three spatial frequencies are shown as marked (0.375, 0.75, and 1.5 cpd at 2 Hz). Axes show contrast normalized by the stimulus detection threshold in the absence of a mask (masked/unmasked thresholds). The data in (A) are fitted with the generalized two-stage model (solid lines) described in the text and weights of within-eye ( $w_m$ ), and between-eye ( $w_o$ ) suppression are estimated from the monocular and dichoptic viewing conditions, respectively. In (B) these two values are used to fit the binocular masking data. The model parameters and goodness of fit are reported in Table 1. Error bars are calculated in terms of Gaussian error propagation (Lo, 2005; Essock, Haun, & Kim, 2009) and the mean of these *SE* are shown.

## Results

Figure 2 shows contrast masking functions for the chromatic stimuli based on the averaged results of all four observers (KTM, JWZ, MG, and YJK), with the individual data for each subject shown in Figure 3. For all functions, threshold elevation is expressed as a proportion of detection threshold measured in the absence of the mask and is plotted as a function of mask contrast, also expressed in threshold units. Averaged data for the monocular and dichoptic presentations are shown in Figure 2A for three spatial frequencies (0.375, 0.75, and 1.5 cpd), and averaged data for the binocular presentations of the same stimuli are shown in Figure 2B. All functions show the presence of masking, with thresholds rising as a function of mask contrast. Some of the individual functions also display facilitation at low suprathreshold mask contrasts. In both the averaged data and in all individual data, the dichoptic condition shows more masking than the monocular (further statistical reports will be provided later). We fitted the data with a model of contrast gain control (solid lines), described below.

## Model

We used a modified “two-stage model” to quantify and compare the relative monocular and dichoptic contributions to XOS in color vision. This model was originally developed to predict monocular and dichoptic masking in achromatic vision for co-oriented test and mask stimuli, which activate within-channel contrast gain controls (Meese & Hess, 2004; Meese, Georgeson, & Baker, 2006), and has subsequently also been successfully applied to XOM (Baker et al., 2007; Meese & Baker, 2009). We chose this model for several reasons. First, it separates the monocular and the binocular stages of visual processing, and we need a model that can potentially be applied to both monocular and binocular thresholds. Second, this model separates the interocular and the monocular (within-eye) sites of XOS occurring prior to binocular summation, allowing us to compare the two. Moreover, a strong case has been made supporting the presence of these two separate sources of suppression (Baker et al., 2007; Meese & Holmes, 2007). However, this model has only previously been used to fit dichoptic and monocular data, and not binocular data. The version of

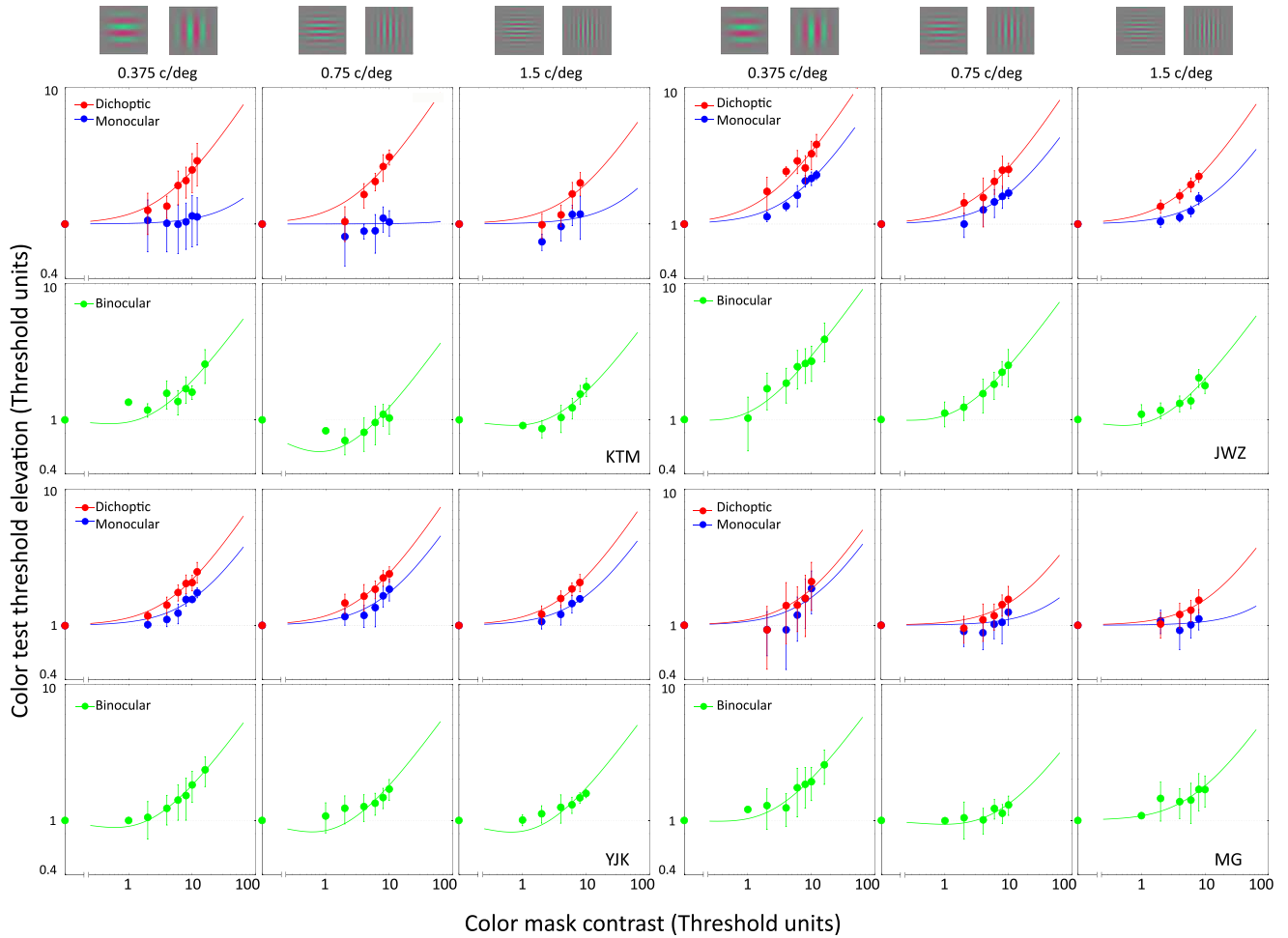


Figure 3. The individual TvC functions for the four subjects used to calculate the averages in Figure 2. All symbols are as for Figure 2.

the two-stage model that we use is illustrated schematically in Figure 4.

The response at the monocular stage (stage 1) prior to binocular summation is given in Equation 2 using the right (R) eye as an example (Meese & Baker, 2009):

$$stage1R = \frac{C_R^m}{S + C_R + C_L + w_m X_R + w_d X_L}, \quad (2)$$

where  $C_L$  and  $C_R$  refer to the contrast of grating stimuli (test or mask) that elicit a response in the left or right eye respectively,  $X_L$  and  $X_R$  refer to the contrast of the cross oriented grating (mask or test) in the left and right eyes respectively,  $w_m$  and  $w_d$  refer to the weight of the within-eye and between-eye cross oriented suppression respectively,  $m$  refers to the excitatory exponent, and  $S$  refers to the saturation constant. Stage 1 is calculated for both test and mask for both eyes.

We are interested in determining  $w_m$  and  $w_d$ , the weights of the XOS. For monocular presentations to the right eye,  $C_L$  and  $X_L$  are 0, and for dichoptic presentations of test to the right eye and mask to the left,  $C_L$  and  $X_R$  are 0. Hence monocular and dichoptic

presentations isolate the within-eye and between-eye suppression sites, respectively.

Binocular summation occurs at the second stage and simply involves summing the left (L) and right (R) eye responses obtained from Equation 2 for test or mask separately. Following the notation of Meese and Baker (2009), binocular summation is given as:

$$binsum_{test} = stage1L_{test} + stage1R_{test} \quad (3a)$$

$$binsum_{mask} = stage1L_{mask} + stage1R_{mask}. \quad (3b)$$

The final output of the model in response to the test is given by inputting the first stage responses into a binocular second stage:

$$resp = \frac{(1 + a \cdot binsum_{mask}) \cdot (binsum_{test})^p}{Z + (binsum_{test})^q + w_b \cdot (binsum_{mask})^q}. \quad (4)$$

The general form of the equation is derived from Foley's Model 3 (Foley, 1994) modified by Meese and Holmes (2007), where the exponents  $p$  and  $q$  represent the rate of acceleration of nonlinear contrast responses on the numerator and denominator of Equation 4,

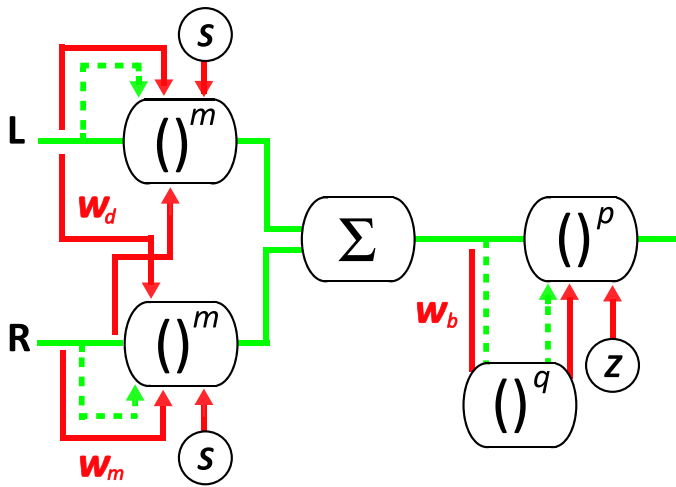


Figure 4. A schematic diagram for the generalized two-stage model used to fit the data. The model is similar to that previously suggested (Meese et al., 2006; Meese & Baker, 2009), but with the addition of one parameter ( $w_b$ , the weight of binocular suppression) to allow binocular viewing conditions as well as monocular and dichoptic to be fitted. Green lines indicate excitatory response lines, red lines indicate suppressive response lines, and the arrows denote divisive input. There is divisive modulatory control in the within-eye (monocular) and interocular (dichoptic) pathways, placed before binocular summation. We used this model to determine the values of the monocular ( $w_m$ , within-eye) and dichoptic ( $w_d$ , interocular) suppression weights and used these to predict the binocular masking condition. Weights of suppression ( $w_m$ ,  $w_d$ , and  $w_b$ ) and facilitation ( $a$ ) are free parameters in the model.

respectively,  $Z$  is a constant of this stage,  $a$  is a parameter that controls the weight of facilitation (Meese & Holmes, 2007), and  $w_b$  is the weight of the binocular, second-stage XOS. The model output differs from that used by Meese and Baker (2009) in that we have included XOS at the binocular stage in addition to the first monocular stage. This is discussed further later. Equation 4 was used to fit all of our data: monocular, dichoptic, and binocular viewing conditions for the three spatial frequencies, for four subjects, and for both chromatic and achromatic stimuli.

In the 2IFC paradigm, detection occurs when the difference between the responses to the *test + mask* and *mask* alone exceeds a criterion value  $k$  (Meese & Holmes, 2007):

$$\text{resp}(\text{test} + \text{mask}) - \text{resp}(\text{mask}) = k, \quad (5)$$

where  $\text{resp}(\text{test} + \text{mask})$  indicates the model response to *mask* and/or *test* (Legge & Foley, 1980). The value  $k$  is proportional to the signal-to-noise ratio that a subject needs to detect the test stimuli at the proportion correct that we measured in our experiment. To solve Equation 4 and fit the masking functions, the test contrast was adjusted until  $\text{resp}(\text{test}) = k$ .

The model contains a total of up to 10 parameters ( $w_m$ ,  $w_d$ ,  $w_b$ ,  $a$ ,  $m$ ,  $S$ ,  $p$ ,  $q$ ,  $Z$ , and  $k$ ). We fixed the values of six of the model parameters based on the relationships in the empirical data and previous work (Meese & Holmes, 2007; Meese & Baker, 2009), as follows:  $m = 1.3$ , which is compatible with empirical binocular summation ratios  $\text{BSR} = 2^{1/m}$  (Baker et al., 2007; Meese & Baker, 2009),  $p = 2.4$ ,  $q = 2$  (Foley, 1994; Meese & Holmes, 2007),  $S = 1$ ,  $k = 0.2$ , and  $Z = 0.7$ . The value  $k$  was obtained by setting the mask contrast equal to 0 in Equation 5 and finding  $\text{resp}(\text{test})$  from Equation 4 for  $C_{\text{test}} = 1$  since we use normalized contrast values in the fit. We adjusted the  $Z$  value to estimate the intercept on the normalized axes, when mask contrast is zero. The values of the remaining parameters were determined from the data using a Matlab *fminsearch* function to optimize the fits.

We fitted the monocular and dichoptic data in Figure 2A first. Each fit had three free parameters:  $a$ ,  $w_b$ , and  $w_m$  for monocular viewing and  $a$ ,  $w_b$ , and  $w_d$  for dichoptic viewing. The fitted values of the within-eye ( $w_m$ ), between-eye ( $w_d$ ), and binocular ( $w_b$ ) weights of suppression and the facilitation weight ( $a$ ) are given in Table 1. The weight of binocular suppression was close to zero and is not included in the table. The goodness of fit of our model was assessed by the adjusted  $R^2$  metric ( $\bar{R}^2$ ) with values given in Table 1 (further details are given in Appendix A).

For the model to have general applicability, it should be able to fit the visual response under binocular conditions when all three sites of suppression are potentially active. We next fitted Equation 4 to our binocular data in Figure 2B. Equation 4 has not been applied previously to binocular data, but only monocular and dichoptic presentations, which do not test the stage of binocular summation (Meese & Baker, 2009). The values of the within-eye ( $w_m$ ) and between-eye ( $w_d$ ) suppression determined from the data in Figure 2A were used to fit the binocular data. The values of the remaining two free parameters ( $a$  and  $w_b$ ) were determined using a Matlab *fminsearch* function to optimize the fits. Other parameters were fixed at  $m = 1.3$ ,  $p = 2.4$ ,  $q = 2$ ,  $S = 1$ ,  $k = 0.2$ , and  $Z = 1.45$  for color and  $Z = 1.8$  for achromatic contrast.  $Z$  was adjusted as before to fit the intercept on the normalized axes and to preserve the same  $k$  value across all conditions. The fitted values of the binocular ( $w_b$ ) weight of suppression and the facilitation weight ( $a$ ) are given in Table 1. The fitted weight of binocular suppression was close to zero. We ascertained that fits obtained with  $w_b$  set to zero are no better than when it is a free parameter, indicating that a reasonable account of the color-masking data can be made without this term as shown in Equation 6 (below). Overall, the results show that the two-stage model provides a reasonable account of the color-masking data in all three viewing conditions.

Subjects	0.375 cpd, 2 Hz			0.75 cpd, 2 Hz			1.5 cpd, 2 Hz		
	Mon	Dic	Bin	Mon	Dic	Bin	Mon	Dic	Bin
	$w_m$	$w_d$	$a$	$w_m$	$w_d$	$a$	$w_m$	$w_d$	$a$
Average subject	0.107	0.352	1.114	0.066	0.269	1.590	0.060	0.208	0.837
KTM	0.015	0.297	0.822	0.001	0.399	4.858	0.024	0.189	0.722
JWZ	0.218	0.541	1.307	0.126	0.332	0.808	0.090	0.300	1.181
YJK	0.101	0.231	1.238	0.136	0.288	1.206	0.119	0.257	1.684
MG	0.108	0.159	0.493	0.017	0.079	0.352	0.010	0.097	0.054
Average of four subjects	0.111	0.307	0.965	0.070	0.275	1.806	0.061	0.211	0.910
SE	0.042	0.083	0.190	0.035	0.069	1.032	0.026	0.044	0.346

Table 1. Fitted model parameters to color contrast data. *Notes:* The table shows the parameter values to three decimal places ( $w_m$ ,  $w_d$ , and  $a$ ) for the model fits to the averaged data of four subjects (Figure 2) and the individual data (Figure 3). Note that the fitted values of the facilitation ( $a$ ) under monocular (Mon) and dichoptic (Dic) conditions and suppression ( $w_b$ ) under the binocular (Bin) condition are close to zero for all masking conditions and so are not included in the table ( $a$  is zero to three decimal places,  $w_b$  is zero to five decimal places). The bottom two rows show the average of the parameter fits across the four subjects and  $\pm 1$  SE of the mean, respectively, which are also plotted in Figures 7 and 8. This model provides a good fit: The adjusted  $R^2$  values for the average subject are 0.914 for monocular, 0.934 for dichoptic, and 0.955 for binocular viewing conditions (averaged across spatial frequency).

$$resp = \frac{(1 + a \cdot binsum_{mask}) \cdot (binsum_{test})^p}{Z + (binsum_{test})^q}. \quad (6)$$

In order to compare chromatic and achromatic masking functions, we obtained a complete set of data for achromatic stimuli, using the same subjects and the same conditions as in Figures 2 and 3. The data sets averaged across the four subjects are shown in Figure 5 in black with the model fit shown by the solid line, and the average functions for the chromatic stimuli shown in red. The individual masking functions for each subject are shown in Figure 6. The model fit parameters for the achromatic stimuli for individual subjects and the fit of the averaged data are given in Table 2. The goodness of the model fits in the averaged achromatic monocular and dichoptic viewing conditions (Figure 5A) are consistent with those for chromatic stimuli, and show a good fit to the data (for color monocular and dichoptic  $R^2$  is 0.914 and 0.934, respectively, and for achromatic monocular and dichoptic  $R^2$  is 0.936 and 0.957, respectively). As before, at each spatial frequency we used the values of  $w_m$  and  $w_d$  obtained from the monocular and dichoptic fits, respectively, in the model fit to the binocular data (Figure 5B). Results show that these fits to the binocular achromatic data are poorer, especially compared to the chromatic binocular condition (averaged  $R^2$ s are 0.955 and 0.759, respectively).

We compare the weights of suppression for color and achromatic XOM under monocular and dichoptic conditions, collapsed across spatial frequency and subject in Figure 7. Monocular suppression ( $w_m$ ) is significantly higher in color compared to achromatic contrast (paired sample  $t$  test:  $t(11) = 3.178$ ,  $p = 0.009$ ), shown in Figure 7A, whereas dichoptic suppression ( $w_d$ ) is similar for both color and achromatic contrast

(paired sample  $t$  test:  $t(11) = 0.879$ ,  $p = 0.398$ ), shown in Figure 7B.

The fitted weights of monocular ( $w_m$ ) and interocular suppression ( $w_d$ ), averaged across four subjects, are plotted across spatial frequency for chromatic and achromatic stimuli in Figure 8A and B, respectively. The color and achromatic data sets (fitted suppression values,  $w_m$  and  $w_d$  for all subjects) were each analyzed using a two-factor repeated-measures ANOVA, with factors of viewing condition and spatial frequency. The main effect of viewing condition is significant for both color,  $F(1, 3) = 13.898$ ,  $p = 0.034$ , and achromatic contrast,  $F(1, 3) = 14.892$ ,  $p = 0.031$ . The planned comparisons tests showed that dichoptic suppression is significantly greater than monocular for both color,  $t(6) = -2.800$ ,  $p = 0.031$ , and achromatic,  $t(6) = -3.577$ ,  $p = 0.012$ , contrast. For color contrast (Figure 8A), there is no significant main effect of spatial frequency,  $F(2, 6) = 1.715$ ,  $p = 0.258$ , and no significant interaction between spatial frequency and viewing condition,  $F(2, 6) = 0.694$ ,  $p = 0.536$ . This shows that suppression obtained from both monocular and dichoptic conditions in color does not depend on spatial frequency over the range used, consistent with previous results reported for binocular color XOM (Medina & Mullen, 2009). For achromatic contrast (Figure 8B), there is also no significant main effect of spatial frequency,  $F(2, 6) = 3.718$ ,  $p = 0.089$ , and no significant interaction between spatial frequency and viewing condition,  $F(2, 6) = 4.429$ ,  $p = 0.066$ , showing that suppression in the monocular and dichoptic conditions of achromatic contrast does not depend on spatial frequency over the range used. A similar result has also been found for achromatic contrast in dichoptic viewing, but not in monocular viewing, which has been shown to depend on speed (i.e., monocular suppression is greater for

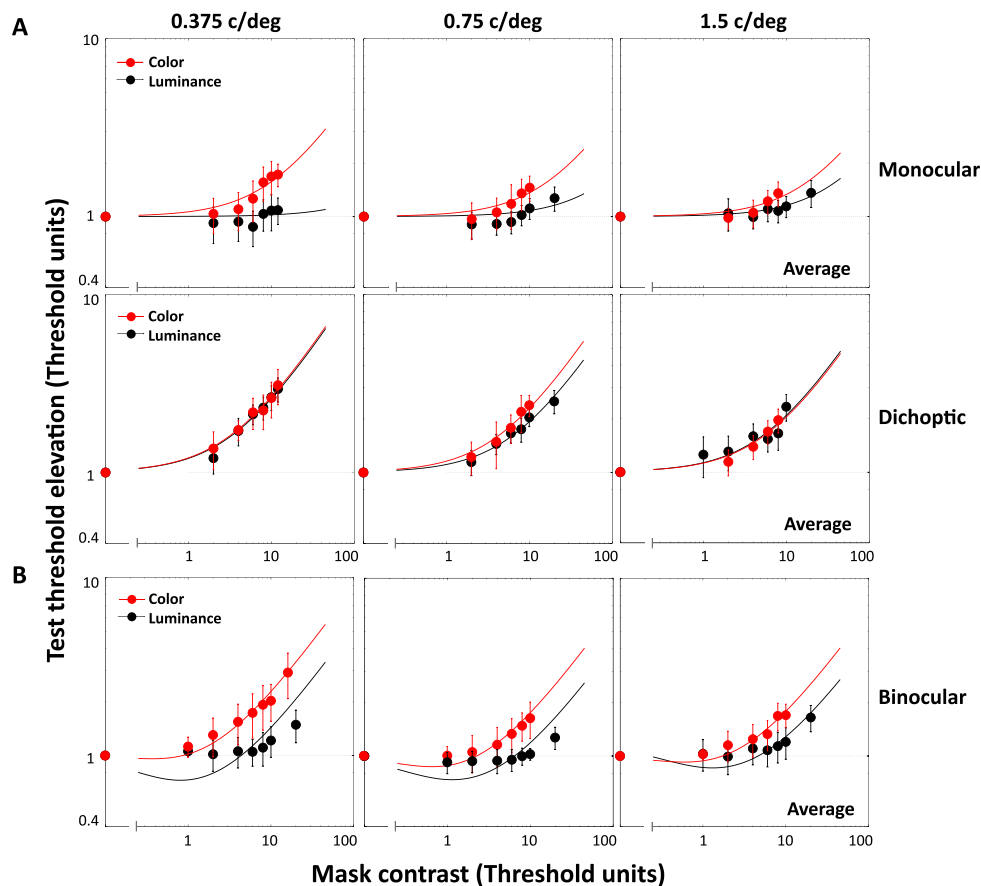


Figure 5. TvC functions for cross-orientation masking are plotted for the chromatic stimuli (red) and for achromatic (black) stimuli for monocular and dichoptic viewing conditions in (A) and binocular viewing conditions in (B). Results are the average across four subjects (KTM, JWZ, MG, and YJK). Chromatic data are the same as for Figure 2. Achromatic data was collected on the same subjects for the same conditions. All data are fitted with the generalized two-stage model (solid lines) as used in previous figures. Model parameters and goodness of fit for the achromatic stimuli are reported in Table 2. Error bars are calculated in terms of Gaussian error propagation and the mean of four *SE* are shown, as in Figure 2.

high temporal frequencies and low spatial frequencies; Meese & Baker, 2009). Our results, however, extend to a lower spatial frequency range (0.375–1.5 cpd at 2 Hz) than was included in this study (0.5–4 cpd at 4 and 15 Hz), which may account for the difference found.

## Discussion

It has been shown for binocular viewing that XOS is greater for color contrast (red-green isoluminant) than for achromatic contrast (Medina & Mullen, 2009). Here we address whether the greater suppression found in binocular color vision originates from a monocular site, an interocular site, or equally from both of these. We measured color XOM under monocular, dichoptic, and binocular conditions and fitted the chromatic masking functions (detection threshold vs. mask

contrast) with a two-stage model developed previously for achromatic contrast (Meese & Hess, 2004; Meese & Baker, 2009). This was done across a range of spatial frequencies. We used this model as a tool to compare the relative strengths of within-eye and between-eye XOS in color vision, and to compare these with the equivalent data obtained for luminance vision. We found that the weight of monocular suppression is significantly greater in color than achromatic contrast, whereas dichoptic suppression is similar for both. These effects are invariant across spatial frequency. We applied the model to the binocular masking data using the measured values of the monocular and interocular sources of suppression and show that these are sufficient to account for color binocular masking. This suggests that the greater strength of chromatic XOM has a monocular origin that transfers through to the binocular site.

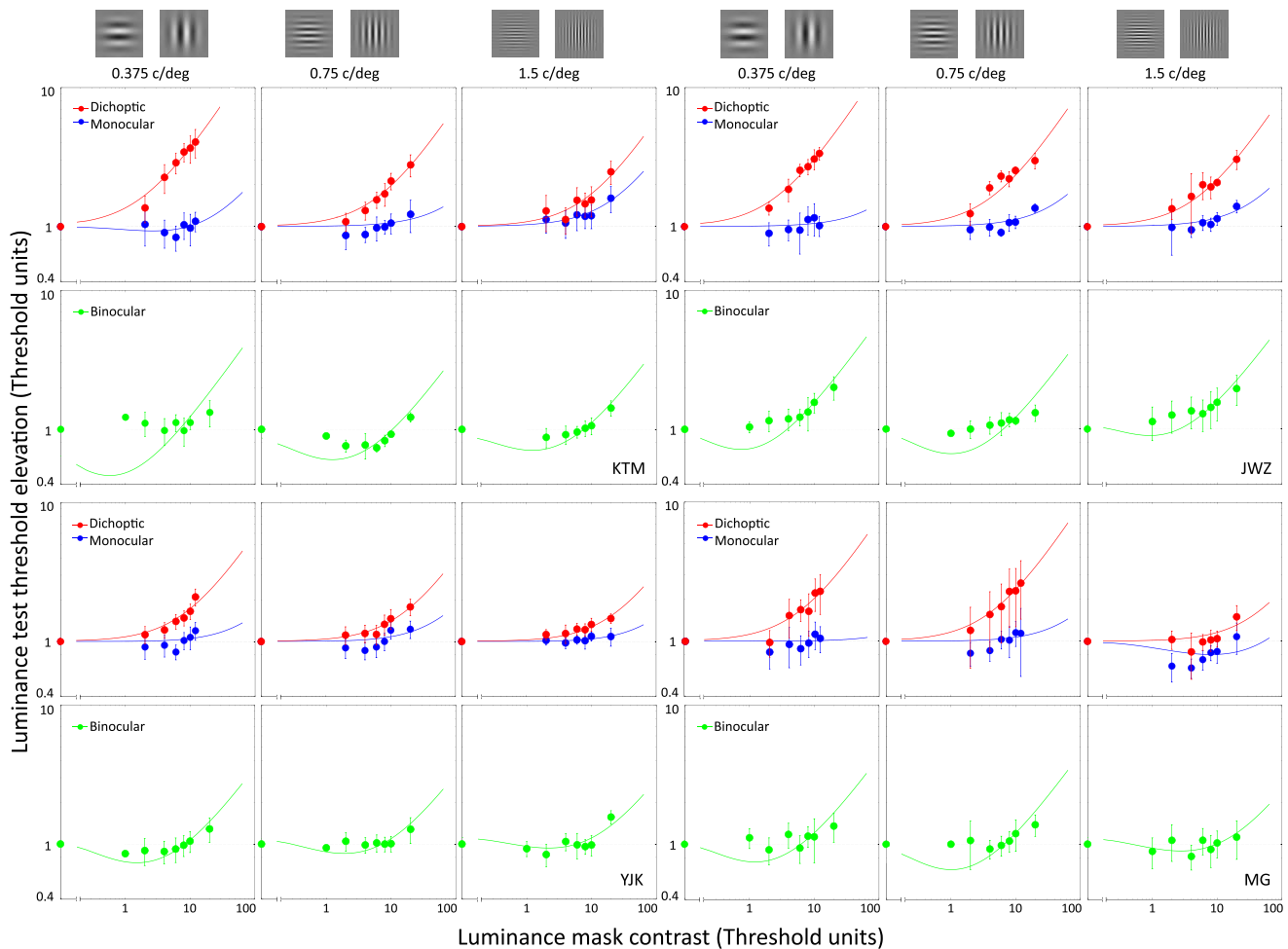


Figure 6. The individual TvC functions for luminance stimuli across the four subjects used to calculate the averages in Figure 5. All symbols are as for Figure 2.

### Application of the two-stage model to color vision

We used this two-stage model (Baker et al., 2007; Meese & Baker, 2009) because it represents each eye separately in the first monocular stage, allowing us to determine the relative contributions of suppression originating within each eye and operating between the eyes, before these inputs are combined into the second binocular stage. The two-stage model was developed for XOM in luminance vision and has not yet been applied to XOM in color vision. Furthermore, in luminance vision it has only previously been used to model monocular and dichoptic viewing conditions and not binocular viewing.

Our results show that the two-stage model can be applied to color XOM in monocular, dichoptic, and binocular conditions, since the model provided a good fit to the data in all these conditions. As we are primarily interested in comparing the two sources of suppression originating prior to binocular summation, we first fitted the model to the monocular and the

dichoptic conditions to extract these weights. In order to test the generality of the model, we used these weights to fit the binocular data. For this, we modified the model to introduce a third weight of suppression at the binocular stage, since suppression is potentially able to occur at both monocular and binocular sites. However, our results showed that the fitted weight of the binocular summation was close to zero under all conditions, and replacing it with actual zero did not alter the fit. This demonstrates that in color vision only two sites of suppression prior to binocular summation are sufficient to account for the binocular data, and this allows us to predict the binocular masking functions. Curiously, when we ran the model on our luminance comparison data, we found that the fit for the binocular data was poorer than we had obtained for the color data. This suggests that the model is less accurate at predicting the binocular masking functions from the two prebinocular sites of suppression in luminance vision and implies other factors or parameters might be involved in luminance XOM.

Subjects	0.375 cpd, 2 Hz					0.75 cpd, 2 Hz					1.5 cpd, 2 Hz				
	Mon		Dic		Bin	Mon		Dic		Bin	Mon		Dic		Bin
	$w_m$	$a$	$w_d$	$a$	$a$	$w_m$	$a$	$w_d$	$a$	$a$	$w_m$	$a$	$w_d$	$a$	$a$
Average subject	0.004	0.000	0.341	0.000	4.349	0.015	0.000	0.170	0.000	2.404	0.027	0.000	0.133	0.000	1.234
KTM	0.001	0.275	0.626	0.000	13.995	0.010	0.000	0.185	0.000	3.607	0.048	0.000	0.133	0.000	2.243
JWZ	0.009	0.002	0.450	0.001	4.083	0.021	0.002	0.270	0.001	3.048	0.026	0.000	0.231	0.000	1.418
YJK	0.011	0.016	0.139	0.014	1.914	0.016	0.016	0.074	0.015	0.724	0.010	0.016	0.050	0.015	0.533
MG	0.002	0.002	0.205	0.001	2.188	0.013	0.008	0.278	0.006	3.808	0.020	0.419	0.028	0.008	0.577
Average of four subjects	0.006	0.073	0.355	0.004	5.545	0.015	0.006	0.202	0.006	2.797	0.026	0.109	0.110	0.006	1.193
SE	0.003	0.067	0.112	0.003	2.858	0.002	0.004	0.047	0.003	0.709	0.008	0.103	0.046	0.004	0.405

Table 2. Fitted model parameters to luminance contrast data. Notes: The table shows the parameter values to three decimal places ( $w_m$ ,  $w_d$ , and  $a$ ) for the model fits to the averaged data of four subjects (Figure 5) and the individual data (Figure 6). Note that the fitted values of the suppression ( $w_b$ ) under the binocular condition are close to zero for all masking conditions and so are not included in the table ( $a$  is zero to three decimal places,  $w_b$  is zero to seven decimal places). The bottom two rows show the average of the parameter fits across the four subjects and  $\pm 1$  SE of the mean, respectively, which are plotted in Figures 7 and 8. The adjusted  $R^2$  values for the average subject are 0.936 for monocular, 0.957 for dichoptic, and 0.759 for the binocular viewing condition (averaged across spatial frequency). The model is a good fit to the monocular and dichoptic data but poorer for the binocular data.

### Greater XOS for color contrast compared to achromatic contrast

We have showed that XOS in color vision is significantly higher than for achromatic contrast, measured under equivalent conditions, and this has a monocular origin not an interocular (dichoptic) one. Specifically, we find that the weight of monocular suppression is significantly higher for color contrast compared to achromatic contrast, whereas the weight of dichoptic suppression is similar in both. This indicates that the greater suppression found for the binocular viewing in color vision, in our data as well as

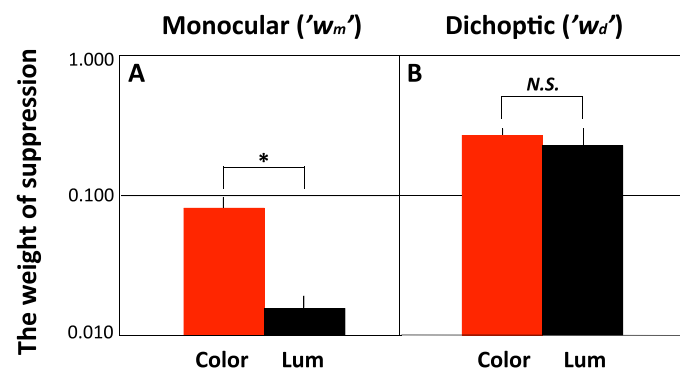


Figure 7. Fitted weights of suppression for monocular ( $w_m$ ) and dichoptic ( $w_d$ ) masking plotted for color (red) and luminance contrast (black). The weights are the average of four subjects collapsed across spatial frequency and error bars are  $\pm 1$  SE of the mean. \*Indicates significant for  $p < 0.05$ . (Values are in Tables 1 and 2.)

in a previous study (Medina & Mullen, 2009), has its origin in a monocular site not an interocular one. In addition, we show that this effect is spatially invariant over the range used, since both chromatic and achromatic XOS for both monocular and dichoptic presentations show no significant dependence on spatial frequency. Previously, Medina and Mullen (2009) have shown that binocular chromatic XOM is invariant across temporal frequency and spatial frequency. For achromatic masking, however, XOM has been shown to be spatiotemporally dependent,

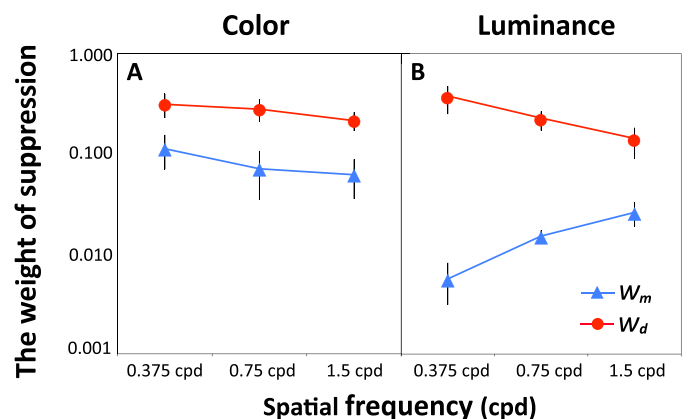


Figure 8. Fitted weights of suppression for monocular ( $w_m$ ) and dichoptic ( $w_d$ ) masking plotted as a function of spatial frequency for chromatic (A) and achromatic (B) contrast. The weights are the average of four subjects and error bars are  $\pm 1$  SE of the mean. The weights of dichoptic suppression are significantly higher than monocular in both cases, and no effect of spatial frequency was found (see text).

with suppression increasing in proportion to stimulus speed, producing the strongest masking at high temporal and low spatial frequencies and weakest masking for low temporal and high spatial frequency conditions (Meier & Carandini, 2002; Meese & Hess, 2004; Cass & Alais, 2006; Meese & Holmes, 2007; Medina & Mullen, 2009). Here our achromatic data do not show an effect of spatial frequency, but we have not directly explored the effect of speed as we have used only one temporal frequency. Comparisons with the results of Meese and Baker (2009) suggest that the effect of spatial frequency is similar in our achromatic data and theirs except that ours extends to a lower spatial frequency range where the effect of spatial frequency is minimal.

The bias of monocular, achromatic XOM for low spatial and high temporal frequencies has led to the suggestion that it originates in the magnocellular pathway or its projections (Meier & Carandini, 2002; Cass & Alais, 2006; Baker et al., 2007; Meese & Holmes, 2007). In contrast, the detection of isoluminant red-green stimuli is based solely on P cell responses and their projections (Derrington, Krauskopf, & Lennie, 1984; Merigan, 1989; Lee, Pokorny, Smith, Martin, & Valberg, 1990; Merigan, Katz, & Maunsell, 1991). Hence, our results demonstrate a strong involvement of the P cell pathway and its projections in XOM, and argue against the idea that M cells are exclusively involved in the mechanism of XOM. In particular, because we find that the color suppression is greatest for the monocular response, a subcortical or early cortical site is suggested. The strength of this chromatic XOM is surprising, however, in view of the reported strong linearity of the contrast response of LGN P cells (Kaplan & Shapley, 1982; Przybyszewski, Gaska, Foote, & Pollen, 2000; Lennie & Movshon, 2005; Solomon & Lennie, 2005), which suggests a lack of contrast normalization in primate LGN P cells, at least for anaesthetized animals. If this is correct, chromatic contrast normalization is likely to be mediated instead in the early stages of cortical processing with intracortical inhibition forming a divisive normalization pool from many other cortical neurons tuned to different preferred orientations (Bonds, 1989; DeAngelis et al., 1992; Heeger, 1992; Carandini & Heeger, 1994; Carandini et al., 1997; Walker et al., 1998; Sengpiel & Vorobyov, 2005). All chromatic neurons in V1 demonstrate normalization (Solomon & Lennie, 2005; Solomon, Lee, & Sun, 2006). Hence, the greater strength of contrast normalization in color vision might be explained by differences in this normalizing gain pool for color versus achromatic contrast. Psychophysical evidence suggests that the underlying orientation tuning of color detectors is somewhat broader than in achromatic vision (Beaudot & Mullen, 2005; Gheiratmand, Meese, & Mullen,

2013). Grating stimuli will cause greater activation of a gain pool if the individual modulatory neurons are broadly rather than narrowly tuned for orientation. Such an effect might potentially contribute to the higher contrast normalization we find for color compared to achromatic contrast. A similar effect might also result from modulatory interactions between isotropic (blob-like) chromatic neurons.

## Differences between monocular and dichoptic masking

Dichoptic suppression ( $w_d$ ) is significantly greater than the monocular suppression ( $w_m$ ) for both color and achromatic contrast. This effect has been found for achromatic contrast (Baker et al., 2007; Meese & Baker, 2009). However, comparisons between dichoptic and monocular suppression have to be made with caution as they have different time dependencies. Dichoptic suppression builds up more slowly in time and its effect may be reduced if shorter presentation times are used (Baker et al., 2007), whereas monocular suppression builds very rapidly. Although we do not yet know the time dependence of dichoptic suppression in color vision, our presentation times are sufficiently long ( $\sigma = 125$  ms) to allow dichoptic suppression to have stabilized, based on achromatic data.

We find that dichoptic suppression is unselective for color, having a similar magnitude for both color and achromatic contrast, whereas monocular suppression shows color selectivity under our conditions. This difference in color selectivity reveals a clear distinction between the processes of interocular and monocular suppression, and adds to other studies demonstrating differences between dichoptic and monocular suppression in achromatic vision, including a differential dependence on time (dichoptic suppression is slower to build up, Baker et al., 2007), on spatial frequency (dichoptic suppression is spatiotemporally invariant), and a differential adaptability with greater adaptation in the dichoptic condition (Li et al., 2005; Sengpiel & Vorobyov, 2005; Li, Thompson, Duong, Peterson, & Freeman, 2006; Baker et al., 2007). This implies two distinct origins for monocular and dichoptic suppression. Dichoptic suppression is thought to involve a cortical site, either by feedback from V1 to the LGN or by intracortical modulation. Modulatory feedback from V1 to the LGN has been demonstrated by many different techniques from anatomical (Sherman & Guillery, 2002), to physiological (Przybyszewski et al., 2000; Webb et al., 2002), to fMRI (O'Connor, Fukui, Pinsk, & Kastner, 2002) and is by far the greatest source of input to the LGN. We find that color is as strong a source of dichoptic suppression as achromatic contrast, although whether this is stream specific or

broadly effective across streams remains to be determined.

*Keywords:* color vision, cross-orientation masking, contrast gain control, dichoptic, psychophysics, isoluminance

## Acknowledgments

We thank Tim Meese and Daniel Baker for early discussion of this work. This research was supported by a Canadian Institutes of Health Research (CIHR) grant MOP-10819 to KTM. We also thank subject Jiawei Zhou (JWZ) for participating in the experiment.

Commercial relationships: none.

Corresponding author: Kathy T. Mullen.

Email: kathy.mullen@mcgill.ca.

Address: McGill Vision Research, Department of Ophthalmology, McGill University, Montreal, Quebec, Canada.

## References

- Baker, D. H., Meese, T. S., & Summers, R. J. (2007). Psychophysical evidence for two routes to suppression before binocular summation of signals in human vision. *Neuroscience*, *146*, 435–448.
- Beaudot, W. H., & Mullen, K. T. (2005). Orientation selectivity in luminance and color vision assessed using 2-d band-pass filtered spatial noise. *Vision Research*, *45*, 687–696.
- Bonds, A. B. (1989). Role of inhibition in the specification of orientation selectivity of cells in the cat striate cortex. *Visual Neuroscience*, *2*, 41–55.
- Brouwer, G. J., & Heeger, D. J. (2011). Cross-orientation suppression in human visual cortex. *Journal of Neurophysiology*, *106*, 2108–2119.
- Carandini, M., & Heeger, D. J. (1994). Summation and division by neurons in primate visual cortex. *Science*, *264*, 1333–1336.
- Carandini, M., Heeger, D. J., & Movshon, J. A. (1997). Linearity and normalization in simple cells of the macaque primary visual cortex. *Journal of Neuroscience*, *17*, 8621–8644.
- Carandini, M., Heeger, D. J., & Senn, W. (2002). A synaptic explanation of suppression in visual cortex. *Journal of Neuroscience*, *22*, 10053–10065.
- Cass, J., & Alais, D. (2006). Evidence for two interacting temporal channels in human visual processing. *Vision Research*, *46*, 2859–2868.
- Cass, J., Stuit, S., Bex, P., & Alais, D. (2009). Orientation bandwidths are invariant across spatiotemporal frequency after isotropic components are removed. *Journal of Vision*, *9*(12):17, 11–14, <http://www.journalofvision.org/content/9/12/17>, doi:10.1167/9.12.17. [PubMed] [Article]
- Cavanagh, P., Tyler, C. W., & Favreau, O. E. (1984). Perceived velocity of moving chromatic gratings. *Journal of the Optical Society of America A*, *1*, 893–899.
- Chen, C. C., & Foley, J. M. (2004). Pattern detection: Interactions between oriented and concentric patterns. *Vision Research*, *44*, 915–924.
- Cole, G. R., Hine, T., & McIlhagga, W. (1993). Detection mechanisms in L-, M-, and S-cone contrast space. *Journal of the Optical Society of America A*, *10*, 38–51.
- DeAngelis, G. C., Robson, J. G., Ohzawa, I., & Freeman, R. D. (1992). Organization of suppression in receptive fields of neurons in cat visual cortex. *Journal of Neurophysiology*, *68*, 144–163.
- Derrington, A. M., Krauskopf, J., & Lennie, P. (1984). Chromatic mechanisms in lateral geniculate nucleus of macaque. *Journal of Physiology*, *357*, 241–265.
- Essock, E. A., Haun, A. M., & Kim, Y. J. (2009). An anisotropy of orientation-tuned suppression that matches the anisotropy of typical natural scenes. *Journal of Vision*, *9*(1):35, 1–15, <http://www.journalofvision.org/content/9/1/35>, doi:10.1167/9.1.35. [PubMed] [Article]
- Foley, J. M. (1994). Human luminance pattern-vision mechanisms: Masking experiments require a new model. *Journal of the Optical Society America A*, *11*, 1710–1719.
- Freeman, T. C., Durand, S., Kiper, D. C., & Carandini, M. (2002). Suppression without inhibition in visual cortex. *Neuron*, *35*, 759–771.
- Geisler, W. S., & Albrecht, D. G. (1992). Cortical neurons: Isolation of contrast gain control. *Vision Research*, *32*, 1409–1410.
- Gheiratmand, M., Meese, T. S., & Mullen, K. T. (2013). Blobs versus bars: Psychophysical evidence supports two types of orientation response in human color vision. *Journal of Vision*, *13*(1):2, 1–13, <http://www.journalofvision.org/content/13/1/2>, doi:10.1167/13.1.2. [PubMed] [Article]
- Heeger, D. J. (1992). Normalization of cell responses in cat striate cortex. *Visual Neuroscience*, *9*, 181–197.
- Holmes, D. J., & Meese, T. S. (2004). Grating and plaid masks indicate linear summation in a contrast gain

- pool. *Journal of Vision*, 4(12):7, 1080–1089, <http://www.journalofvision.org/content/4/12/7>, doi:10.1167/4.12.7. [PubMed] [Article]
- Kaplan, E., & Shapley, R. M. (1982). X and Y cells in the lateral geniculate nucleus of macaque monkeys. *Journal of Physiology*, 330, 125–143.
- Lee, B. B., Pokorny, J., Smith, V. C., Martin, P. R., & Valberg, A. (1990). Luminance and chromatic modulation sensitivity of macaque ganglion cells and human observers. *Journal of the Optical Society of America A*, 7, 2223–2236.
- Legge, G. E., & Foley, J. M. (1980). Contrast masking in human vision. *Journal of the Optical Society of America*, 70, 1458–1471.
- Lennie, P., & Movshon, J. A. (2005). Coding of color and form in the geniculostriate visual pathway (invited review). *Journal of the Optical Society of America A: Optics, Image Science, & Vision*, 22, 2013–2033.
- Li, B., Peterson, M. R., Thompson, J. K., Duong, T., & Freeman, R. D. (2005). Cross-orientation suppression: Monoptic and dichoptic mechanisms are different. *Journal of Neurophysiology*, 94, 1645–1650.
- Li, B., Thompson, J. K., Duong, T., Peterson, M. R., & Freeman, R. D. (2006). Origins of cross-orientation suppression in the visual cortex. *Journal of Neurophysiology*, 96, 1755–1764.
- Lo, E. (2005). Gaussian error propagation applied to ecological data: Post-ice-storm-downed woody biomass. *Ecology Monographs*, 75, 451–466.
- Medina, J. M., & Mullen, K. T. (2009). Cross-orientation masking in human color vision. *Journal of Vision*, 9(3):20, 1–16, <http://www.journalofvision.org/content/9/3/20>, doi:10.1167/9.3.20. [PubMed] [Article]
- Meese, T. S., & Baker, D. H. (2009). Cross-orientation masking is speed invariant between ocular pathways but speed dependent within them. *Journal of Vision*, 9(5):2, 1–15, <http://www.journalofvision.org/content/9/5/2>, doi:10.1167/9.5.2. [PubMed] [Article]
- Meese, T. S., Georgeson, M. A., & Baker, D. H. (2006). Binocular contrast vision at and above threshold. *Journal of Vision*, 6(11):7, 1224–1243, <http://www.journalofvision.org/content/6/11/7>, doi:10.1167/6.11.7. [PubMed] [Article]
- Meese, T. S., & Hess, R. F. (2004). Low spatial frequencies are suppressively masked across spatial scale, orientation, field position, and eye of origin. *Journal of Vision*, 4(10):2, 843–859, <http://www.journalofvision.org/content/4/10/2>, doi:10.1167/4.10.2. [PubMed] [Article]
- Meese, T. S., & Holmes, D. J. (2007). Spatial and temporal dependencies of cross-orientation suppression in human vision. *Proceedings of the Biological Sciences*, 274, 127–136.
- Meese, T. S., Summers, R. J., Holmes, D. J., & Wallis, S. A. (2007). Contextual modulation involves suppression and facilitation from the center and the surround. *Journal of Vision*, 7(4):7, 1–21, <http://www.journalofvision.org/content/7/4/7>, doi:10.1167/7.4.7. [PubMed] [Article]
- Meier, L., & Carandini, M. (2002). Masking by fast gratings. *Journal of Vision*, 2(4):2, 293–301, <http://www.journalofvision.org/content/2/4/2>, doi:10.1167/2.4.2. [PubMed] [Article]
- Merigan, W. H. (1989). Chromatic and achromatic vision of macaques: Role of the P pathway. *Journal of Neuroscience*, 9, 776–783.
- Merigan, W. H., Katz, L. M., & Maunsell, J. H. (1991). The effects of parvocellular lateral geniculate lesions on the acuity and contrast sensitivity of macaque monkeys. *Journal of Neuroscience*, 11, 994–1001.
- Morrone, M. C., Burr, D. C., & Maffei, L. (1982). Functional implications of cross-orientation inhibition of cortical visual cells. I. Neurophysiological evidence. *Proceedings of the Royal Society of London B: Biological Sciences*, 216, 335–354.
- O'Connor, D. H., Fukui, M. M., Pinsk, M. A., & Kastner, S. (2002). Attention modulates responses in the human lateral geniculate nucleus. *Nature Neuroscience*, 5, 1203–1209.
- Petrov, Y., Carandini, M., & McKee, S. (2005). Two distinct mechanisms of suppression in human vision. *Journal of Neuroscience*, 25, 8704–8707.
- Priebe, N. J., & Ferster, D. (2006). Mechanisms underlying cross-orientation suppression in cat visual cortex. *Nature Neuroscience*, 9, 552–561.
- Przybylski, A. W., Gaska, J. P., Foote, W., & Pollen, D. A. (2000). Striate cortex increases contrast gain of macaque LGN neurons. *Visual Neuroscience*, 17, 485–494.
- Ross, J., & Speed, H. D. (1991). Contrast adaptation and contrast masking in human vision. *Proceedings of the Biological Sciences*, 246, 61–69.
- Sankeralli, M. J., & Mullen, K. T. (1996). Estimation of the L-, M- and S-cone weights of the post-receptoral detection mechanisms. *Journal of the Optical Society of America A*, 13, 906–915.
- Sengpiel, F., & Vorobyov, V. (2005). Intracortical

origins of interocular suppression in the visual cortex. *Journal of Neuroscience*, 25, 6394–6400.

- Sherman, S. M., & Guillery, R. W. (2002). The role of the thalamus in the flow of information to the cortex. *Philosophical Transactions of the Royal Society of London B: Biological Science*, 357, 1695–1708.
- Smith, V. C., & Pokorny, J. (1975). Spectral sensitivity of the foveal cone photopigments between 400 and 500 nm. *Vision Research*, 15, 161–171.
- Solomon, S. G., Lee, B. B., & Sun, H. (2006). Suppressive surrounds and contrast gain in magnocellular-pathway retinal ganglion cells of macaque. *Journal of Neuroscience*, 26, 8715–8726.
- Solomon, S. G., & Lennie, P. (2005). Chromatic gain controls in visual cortical neurons. *Journal of Neuroscience*, 25, 4779–4792.
- Truchard, A. M., Ohzawa, I., & Freeman, R. D. (2000). Contrast gain control in the visual cortex: Monocular versus binocular mechanisms. *Journal of Neuroscience*, 20, 3017–3032.
- Walker, G. A., Ohzawa, I., & Freeman, R. D. (1998). Binocular cross-orientation suppression in the cat's striate cortex. *Journal of Neurophysiology*, 79, 227–239.
- Webb, B. S., Tinsley, C. J., Barraclough, N. E., Easton, A., Parker, A., & Derrington, A. M. (2002). Feedback from V1 and inhibition from beyond the classical receptive field modulates the responses of neurons in the primate lateral geniculate nucleus. *Visual Neuroscience*, 19, 583–592.

## Appendix A

**Fit of the model.** The goodness of fit of the model, shown in Tables 1 and 2 for color and luminance, respectively, was assessed by the adjusted  $R^2$  metric ( $\bar{R}^2$ ) that measures the variance between model and data normalized to the observed variance and adjusted by the degrees of freedom. The error calculated by this metric is typically between 0 and 1, with near 1.0 value indicating a good fit for the observed data for the degrees of freedom used. The adjusted  $R^2$  can be calculated as:

$$\begin{aligned}\bar{R}^2 &= 1 - \frac{SS_{err}}{SS_t} \cdot \frac{df_t}{df_e} \\ &= 1 - \sum_{i=1:n} \left( \frac{model(i) - data(i)}{\sigma(i)} \right)^2 \cdot \frac{df_t}{df_e},\end{aligned}$$

where  $SS_t$  indicates the variance of the data set that is measured through the sum of squared difference between mean and observed data,  $SS_{err}$  indicates the variance between model and observed data that is measured through the sum of squared difference between model and data,  $n$  is the number of data points,  $df_t$  is the degrees of freedom  $n - 1$  of the estimate of the population variance of the model parameter, and  $df_e$  is the degrees of freedom  $n - p - 1$  of the estimate of the underlying error variance from the data set, with  $p$  being the number of free parameters. Note that there are two free parameters in the binocular condition, whereas there are three free parameters in both monocular and dichoptic conditions, and the number of data points measured are different under each condition. Thereby the adjusted  $R^2$  metric is more accurate than  $R^2$ .